0026-895X/99/030594-11$3.00/0

MOLECULAR PHARMACOLOGY, **55:**594–604 (1999).

Regulation of Cytochrome P-450 (CYP) 1B1 in Mouse Hepa-1 Variant Cell Lines: A Possible Role for Aryl Hydrocarbon Receptor Nuclear Translocator (ARNT) as a Suppressor of *CYP1B1* Gene Expression

SAKINA E. ELTOM, LEYING ZHANG, and COLIN R. JEFCOATE

Center for Environmental Toxicology and Department of Pharmacology, University of Wisconsin Medical School, Madison, Wisconsin

Received April 27, 1998; accepted November 19, 1998

This paper is available online at http://www.molpharm.org

ABSTRACT

Cytochrome P-450 (CYP) 1B1 expression in mouse hepatoma (Hepa-1) wild-type (WT) cells was compared with responses in Hepa-1 variants LA1 and LA2, which, respectively, exhibit low aryl hydrocarbon receptor (AhR) level and defective AhR nuclear translocator (ARNT) protein. 10T1/2 mouse embryo fibroblasts express predominantly CYP1B1 and at a 100 times higher level than in Hepa-1 cells, whereas they express about 300-fold lower CYP1A1 than Hepa-1 cells. The expression of CYP1B1 in WT and LA1 variant, although at a much lower level, follows that of CYP1A1, reflecting their common regulation through the AhR. The LA2 (ARNT-defective) cells showed a major difference between CYP1B1 and CYP1A1 expression. Although CYP1A1 mRNA levels in LA2 were extremely low and unresponsive to 2,3,7,8-tetrachlorodibenzo-*p*-dioxin (TCDD), basal CYP1B1 mRNA and protein were expressed at levels similar to those seen in TCDD-induced WT. The elevated basal CYP1B1 mRNA in LA2 cells decreased by 50% after transient transfection of ARNT cDNA, in parallel with substantial restoration of CYP1A1 induction. This implicates ARNT as a suppressor of CYP1B1 basal expression in Hepa cells. In transient CYP1B1-luciferase constructs in LA2 cells, ARNT shows stimulatory effects in the enhancer region but an inhibitory effect on the proximal promoter. Two CYP1B1 enhancer elements [xenobiotic-responsive element (XRE) 1/2 and XRE4] formed TCDD-unresponsive complexes of similar mobility to TCDD-stimulated AhR-ARNT complex with XRE5. However, because these two complexes were formed to the same extent in LA2 as in WT cells, they cannot be due to ARNT or contribute to ARNT-regulated suppression.

Work in this laboratory has led to the identification of a new form of cytochrome P-450 (CYP) in embryo fibroblasts and steroidogenic tissues (Pottenger and Jefcoate 1990; Otto et al., 1991) that is induced by polycyclic aromatic hydrocarbons (PAH). Cloning and characterization of the genes encoding this P-450 form was reported in rats, mice, and humans (Shen et al., 1993; Savas et al., 1994; Sutter et al., 1994; Bhattacharyya et al., 1995), and based on amino acid sequence homology with CYP1A1 (40%), this gene has been designated *CYP1B1*. Like CYP1A1, CYP1B1 is very active in the metabolism of PAHs but exhibits distinct regioselectivity, particularly for 7,12-dimethylbenz[*a*]anthracene (DMBA). In rodents, CYP1B1 produces the 3,4- and 10,11-dihydrodiols as major products, which are almost absent with CYP1A1 (Pottenger et al., 1991; Savas et al., 1997). An important implication for this difference in product formation is that CYP1B1 is more effective than CYP1A1 in converting DMBA to the ultimate carcinogenic 3,4-dihydrodiol 1,2-epoxide (Wislocki et al., 1980). CYP1B1 represents the predominant PAH-metabolizing P-450 in rodent embryo and mammary fibroblasts and the mouse embryo fibroblast 10T1/2 cell lines. CYP1B1 also is coexpressed with CYP1A1 in mesodermal epithelial cells (skin and breast), although CYP1B1 predom-

This work was supported by National Institutes of Health Grant CA16265. S.E.E. is supported by Grant T32 ES07015 from the National Institute of Environmental Health Sciences, National Institutes of Health and Contribution #323; Environmental Toxicology Center, University of Wisconsin, Madison, WI 53706. Part of this work was presented at the XI International Symposium on Microsomes and Drug Oxidations, Los Angeles, CA, July 21–24, 1996, and part of it was presented at the 37th Society of Toxicology Annual Meeting, Seattle, WA, March 1–5, 1998.

ABBREVIATIONS: PAH, polycyclic aromatic hydrocarbon; AhR, aryl hydrocarbon receptor; ARNT, AhR nuclear-translocating protein; Hepa-1, mouse hepatoma cell line; WT, wild type; LA1, low aryl hydrocarbon hydroxylase activity, class I variant; LA2, low aryl hydrocarbon hydroxylase activity, class II variant; CYP, cytochrome P-450; TCDD, 2,3,7,8-tetrachlorodibenzo-*p*-dioxin; BA, benz[*a*]anthracene; DMBA, 7,12-dimethylbenz[*a*]anthracene; RT-PCR, reverse transcription-polymerase chain reaction; GAPDH, glyceraldehyde-3-phosphate dehydrogenase; ECL, enhanced chemiluminescence; XRE, xenobiotic-responsive element; EMSA, electrophoretic mobility-shift assay; bHLH, basic helix-loop-helix; DTT, dithiothreitol.

inates under basal conditions. This preferential display of CYP1B1 has prompted questions about the cell-specific regulation of these two genes (Christou et al., 1995; Eltom et al., 1998).

The better inducibility of CYP1B1 protein by benz[*a*]anthracene (BA) than by 2,3,7,8-tetrachlorodibenzo-*p*-dioxin (TCDD), the strongest Ah receptor (AhR) agonist (Savas and Jefcoate, 1994), and the observation that CYP1B1 and not CYP1A1 was expressed constitutively in livers of AhR knockout mice (Ryu et al., 1996) raise the question of whether induction of CYP1B1 by PAHs is solely via AhR. The AhR, which is a ligand-activated basic helix-loop-helix (bHLH) transcriptional factor (Burback et al., 1992), binds PAHs and mediates their biological responses, including induction of drug-metabolizing enzymes. The action of AhR in the induction of CYP1A1 has been studied extensively and has established the role of a functional ligand-receptor complex in the expression of CYP1A1 (Legraverend et al., 1982; Jones et al., 1985). The binding of inducers to AhR results in its transformation into a form that readily forms a heterodimer in the nucleus with the related bHLH, ARNT protein (Hoffman et al., 1991). Binding of the receptor complex to DNA-recognition motifs designated as xenobiotic-responsive elements (XREs) results in enhanced transcription of multiple genes, including *CYP1A1* (Denison et al., 1989). Studies in this laboratory have identified an enhancer region with five conserved, putative XREs in the upstream 5′ flanking sequence of *CYP1B1* gene (Zhang et al., 1998) that closely resembles a similarly located enhancer region in *CYP1A1* gene.

From the mouse hepatoma cell line, Hepa variants low activity class 1 (LA1) and low activity class 2 (LA2) were derived as benzo[*a*]pyrene-resistant variants of mouse hepatoma (Hepa-1)c1c7 (WT) and were identified based on their failure to induce aryl hydrocarbon hydroxylase activity (Legraverend et al., 1982; Miller et al., 1983; Hankinson et al., 1985) in response to PAH treatment. LA1 cells have been reported variously to express only 10% of WT AhR and CYP1A1 mRNA levels (Legraverend et al., 1982; Miller et al., 1983). The LA2 variant, which has no detectable basal or inducible aryl hydrocarbon hydroxylase activity, contains a normal cytosolic AhR, but fails to translocate the receptor to the nucleus because of a defective *ARNT* gene (Hoffman et al., 1991).

In the present work we used the Hepa-1 cell lines to investigate the role of AhR and ARNT in regulating CYP1B1 in relation to CYP1A1. The use of reverse transcription-polymerase chain reaction (RT-PCR) method for quantitation of the low CYP1B1 expression in these epithelial cells has allowed us to address further the question of cell specificity in CYP expression. The activity of luciferase-reporter constructs that use various *CYP1B1* promoter sequences has been examined in LA2 and WT cells to assess their regulation by ARNT. Transient transfection of ARNT cDNA in LA2 cells has provided the means to directly examine the role of ARNT in modulating the transcription of *CYP1B1* in Hepa-1 cell lines. We have probed nuclear extracts from WT and LA2 cells in electrophoretic mobility-shift assays (EMSAs) with oligonucleotides corresponding to various *CYP1B1* putative XREs, and the contribution of ARNT to these complexes has been assessed with anti-ARNT antibodies. Evidence for an unusual participation of ARNT-like proteins in *CYP1B1* regulation is presented.

Materials and Methods

Cell Culture and Treatments. Mouse hepatoma cell lines, Hepa-1 WT, and class I and II mutants (LAI and LA2) were the kind gift of Dr. James Whitlock, Jr. (Stanford University, Stanford, CA). Cells were maintained in Dulbecco's modified Eagle's medium with high glucose and 5% heat inactivated fetal bovine serum, 100 U/ml penicillin, 100 μg/ml streptomycin, and 2.5 μg/ml amphotericin B as fungizone. All cultures were maintained in a humidified atmosphere containing 5% CO_2 and 95% air, at 37°C. Cells were treated at subconfluency with 10 μM BA, 10 nM TCDD, or an equivalent volume of DMSO to a final 0.1% concentration (vehicle control) for the indicated times. Cells that were used for RNA isolation and analysis were lysed directly in Trizol reagent after removal of the treatment media. Alternatively, cells were harvested after treatment, by mechanical scraping into cold PBS, and pelleted by centrifugation, and cell pellets were washed in PBS and used to prepare microsomes for Western blotting and DMBA metabolism.

RNA Isolation and RT-PCR Analysis. A quantitative RT-PCR assay was developed to measure the level of induction of both CYP1B1 and CYP1A1 mRNA levels. Total cellular RNA was prepared from control or treated cells by an improved method using the Trizol reagent (Chomcynski, 1993). To remove the possible genomic DNA contamination, all RNA samples were treated with RNase-free DNase (Promega, Madison, WI) in the presence of 10 mM $MgCl_2$ and 0.1 mM dithiothreitol (DTT) for 1 h at 37°C. RNA was then double-extracted in phenol/chloroform and precipitated with acidic sodium acetate and ethanol. cDNA templates for PCR were synthesized from total RNA by reverse transcription as follows: 1 μg of total RNA in diethyl-pyrocarbonate-treated water was annealed with 0.5 μg nanomer random primers at 65°C for 5 min, then cooled slowly to room temperature. Reverse transcription was carried out in a total volume of 25 μl and a final buffer concentration of 50 mM Tris-HCl (pH 8.3), 75 mM KCl, 3 mM $MgCl_2$, 10 mM DTT, 1 mM each of dATP, dGTP, dCTP, dTTP, 25 units of placental RNase inhibitor, and 200 U of murine Moloney leukemia virus reverse transcriptase (Promega). Samples then were incubated at 40°C for 1 h, and the reaction was terminated by heating the samples at 95°C for 5 min. PCR primers for CYP1B1 and CYP1A1 were designed based on the mouse cDNA sequences of these two genes (Table 1) and were synthesized with an Applied Biosystems 380A synthesizer. Primers for glyceraldehyde 3-phosphate dehydrogenase (GAPDH), which were designed to am-

TABLE 1

Oligonucleotide primers and conditions for PCR amplification of cDNA fragments of CYP1A1 and CYP1B1

RNA was isolated from cultured mouse Hepa-1 cell lines (WT and variants) using Trizol reagent and subjected to RT to obtain cDNA. Aliquots of cDNA were amplified by PCR using these primers and according to conditions described below.

Primers	Location on Respective cDNA	Sequence
Forward-CYP1B1	753–774	5′-GATCCAACGCCGCCGGTCATTG-3′
Reverse-CYP1B1	1077–1098	5′-GCCCAAAAGAAAGCGTCTGGGG-3′
Forward-CYP1A1	249–268	5′-TTGCCCTTCATTGGTCACAT-3′
Reverse-CYP1A1	739–758	5′-GAGCAGCTCTTGGTCATCAT-3′
Forward-GAPDH	586–605	5′-ACCACAGTCCATGCCATCAC-3′
Reverse-GAPDH	1018–1037	5′-TCCACCACCCTGTTGCTGTA-3′

plify the region between 586 and 1037 of GAPDH cDNA sequence, were obtained commercially from Clontech (Palo Alto, CA) .

PCR conditions were optimized using these sets of primers and plasmid vectors, which carry the respective cDNA of CYP1B1 and CYP1A1 as templates (Table 1). In each PCR experiment, water was used as a template (no DNA) to control for background contamination while GAPDH cDNA was amplified as an internal standard to normalize quantitation. Simultaneous PCR amplification of GAPDH did not interfere with CYP1B1 or CYP1A1 amplification. The PCR product of each of these genes was quantitated during the exponential phase of amplification. For this purpose, PCR amplifications were carried out after serial dilution of cDNA samples and variation of the number of amplification cycles. To verify the identity of the PCR-amplified fragments, the PCR products were electrophoresed on agarose gels, transferred to nylon membranes, and hybridized with ^{32}P-labeled cDNA probes for, respectively, CYP1B1 (1028-bp mouse cDNA, *Eco*RI-*Hin*dIII, 2×10^6 cpm/ml, 16 h at 42°C) (Savas et al., 1994), full-length mouse CYP1A1 cDNA probe (1×10^6 cpm/ml, 16 h at 42°C) (Gonzalez et al., 1984), and full-length GAPDH cDNA (1×10^6 cpm/ml, 16 h at 42°C) (Fort et al., 1985).

In each PCR experiment, cDNA samples containing the expected highest level of expression were serially diluted and PCR-amplified to generate a standard (calibration) curve (Fig. 1). Serially diluted cDNA (calibration dilutions) or the diluted unknown cDNA was PCR-amplified in a final reaction volume of 25 μl using the Perkin-Elmer thermal cycler according to the conditions listed in Table 2. Aliquots of the PCR products were electrophoresed on 1.5% agarose gels and visualized with ethidium bromide staining. Negative images of gels were generated using Type 55 Polaroid films. These images were scanned and translated into TIFF-formatted files using a Hewlett-Packard ScanJet 3p scanner (Palo Alto, CA) and Adobe Photoshop software (Adobe Systems Inc., Mountain View, CA). The intensity of the bands were quantified using the NIH-image analysis computer program. The integrated area under the curve representing the optical intensity of each band, measured in pixels, was plotted against the dilution of the corresponding cDNA template to generate calibration curves as shown in Fig. 1. The relative level of each amplified unknown sample (hence, the level of the initial RNA expression) is calculated from the calibration curve and normalized for its relative GAPDH levels. Only the linear range of the curve (at high dilution) was used, and unknown cDNA samples were diluted before PCR amplification to fit within this range.

TABLE 2

Conditions that varied among three amplified cDNAs

The rest of the PCR conditions are similar for all three cDNAs and were carried out as described in *Materials and Methods*. Amplification of CYP1B1 and GAPDH was carried out simultaneously; first, CYP1B1 primers were added and samples were amplified for 15 cycles, then cycler was stopped and GAPDH primers and fresh *Taq* polymerase were added and reaction resumed for an extra 20 cycles.

PCR Conditions	CYP1B1	CYP1A1	GAPDH
Primer concentration	250 nM each	400 nM each	250 nM each
Number of cycles	35	25	20
Annealing temperature	60°C	56°C	60°C

Isolation of Cellular Proteins for AhR and ARNT Measurements. Cells were harvested under denaturing conditions by lysing them directly in Trizol. Trizol lysate was used for isolation of total cellular proteins after the consecutive isolation of both total cellular RNA and DNA. Proteins first were precipitated with isopropanol, followed by multiple washes of protein pellets with guanidine-HCl solution in 95% ethanol. Final protein pellets were dried from 100% ethanol and solubilized by sonication in 2% SDS. Protein concentration was determined by the bicinchoninic acid method (Smith et al., 1985).

Transfection and Luciferase Assay. The *CYP1B1* 5′ deletion constructs linked to the luciferase reporter gene were designed as described in previous studies (Zhang et al., 1998). Cells were cultured in Dulbecco's modified Eagle's medium/F12 medium supple-

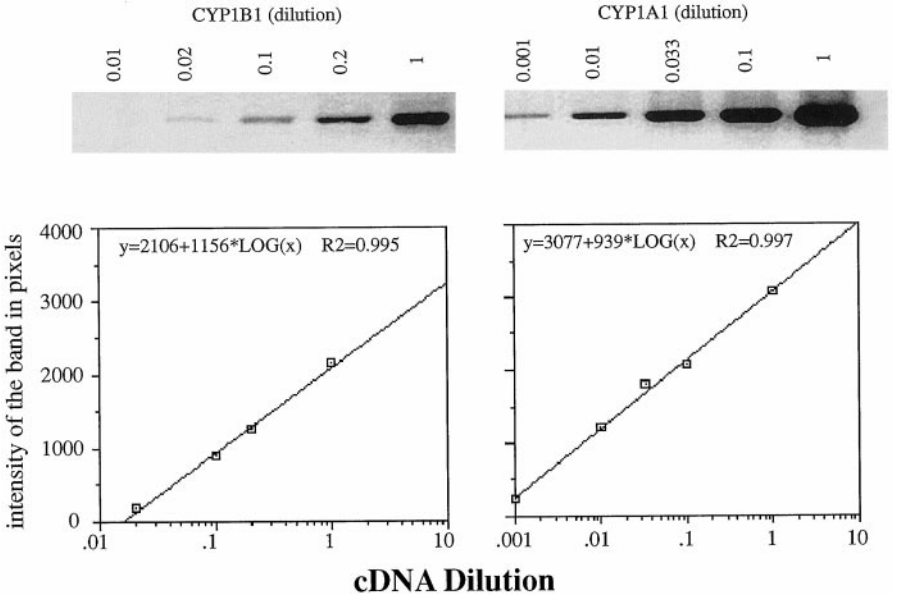

Fig. 1. Calibration curve for quantitation of CYP1A1 and CYP1B1 mRNA by RT-PCR. Each point is average of duplicate PCR. PCR products of serially diluted cDNA samples were electrophoresed on 1.5% agarose gel, and negative film images of gel were scanned digitally to quantify optical density (OD) of bands. Calculated OD of each band was plotted against logarithmic value of corresponding cDNA dilution to generate standard curves. Regression-analysis equation of curve was used to calculate relative dilution of tested samples, which were run simultaneously.

TABLE 3

Oligonucleotides (30-mer) used in gel mobility-shift experiments

Positions of XREs relative to transcription initiation site and their sequences are listed. Regions that match CACGC or CACGCAA motifs are underlined. E-box motif CAGGTG is double-underlined.

Element	Sequence	Position
XRE1/XRE2	CGGCAGCTGTGCGTGCGCCGCCAAGGGTGG	−1033/−1004
XRE3	GCCGCCGCCTCGGCGTGTCAGGTGTCGTGA	−980/−951
XRE4	AGAAGCGGCGCACGCAAGGCACAGCTCCGC	−890/−861
XRE5	ACAGCTCCGCACGCAAGGGGGAGGCGACAG	−870/−841

mented with 5% fetal bovine serum. All plasmids containing constructs and either plasmid pmARNT containing murine ARNT cDNA or the vector plasmids were cotransfected by electroporation method using Gene Pulser apparatus with Capacitance Extender (Bio-Rad, Hercules, CA), according to a modified manufacturer's protocol: five million cells were harvested by trypsinization and dispersed to a single-cell suspension in PBS. Cells in a total of 0.4 ml volume then were placed in the electroporation cuvette, and 10 μg DNA of ARNT cDNA or its vector were added in addition to 4 μg DNA of recombinant reporter constructs. The β-galactosidase expression vector pCH110 was cotransfected to normalize for transfection efficiency. Cells were pulsed at 4°C for 30 s at these machine settings: 0.3 kV, 1.5 kV/cm field strength, and 960-μF capacitors with no resistor. Cells then were plated in six-well plates for either luciferase activity measurements or RNA isolation and subsequent RT-PCR analysis. Cells were allowed to grow for 24 h in their regular culture medium, and then they were treated with 1 nM TCDD or DMSO for 24 h. Luciferase activity was determined using the luciferase assay kit (Promega, Madison, WI) according to the manufacturer's instructions, and luciferase activity was measured immediately in a luminometer.

EMSA. The EMSA was performed using the oligos listed in Table 3 as DNA probes. Nuclear extracts were prepared from control and TCDD-induced (1 nM for 2 h) Hepa-1 WT or LA2 variant lines. The preparation of nuclear extracts and ^{32}P-labeling of DNA using T4 polynucleotide kinase were as described previously (Zhang et al., 1998). In addition, parallel binding was run in the presence of either purified anti-AhR IgGs or anti-ARNT IgGs, where these antibodies were incubated after oligo binding to nuclear extracts.

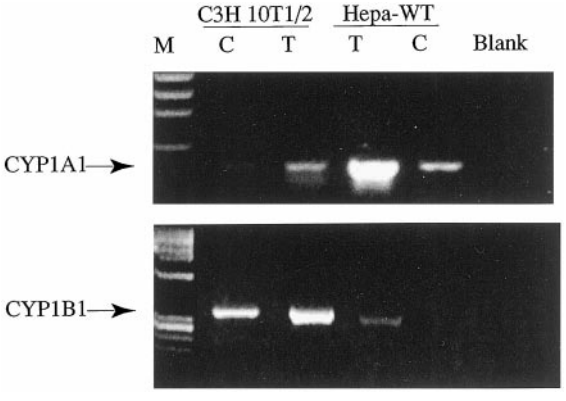

Fig. 2. RT-PCR analysis of relative expression of CYP1A1 and CYP1B1 in WT Hepa-1 cell lines and C3H10T1/2 mouse embryo fibroblast cell lines. Cells were treated with 10 nM TCDD or DMSO for 20 h, and total RNA was isolated by Trizol method. Aliquots of RNA samples were subjected to RT-PCR analysis for CYP1A1 and CYP1B1 expression. Shown is a representative image of ethidium bromide-stained gel of PCR-amplified products of CYP1A1 (25 cycles) and CYP1B1 (30 cycles). These gel images were quantified to obtain values presented in Table 4.

TABLE 4

Comparison of relative levels of constitutive and TCDD-induced CYP1A1 and CYP1B1 mRNA and proteins in Hepa-1 and 10T1/2 cell lines

		CYP1A[a]		CYP1B1[b]	
		Control	TCDD	Control	TCDD
10T1/2	mRNA	1	14 (14)[d]	93	2059 (21)[d]
	Protein[c]				30
Hepa-WT	mRNA	30	5284 (170)[d]	1	18 (18)[d]
	Protein[c]	0.04	25	0.02	0.15

[a] Relative to mRNA levels in untreated 10T1/2 cell line.
[b] Relative to untreated Hepa-1.
[c] pmole CYP per milligram microsomal proteins.
[d] Numbers in parentheses are folds of induction relative to respective untreated control.

Enzyme Activity in Whole Cells in Culture. DMBA metabolism in whole cells was measured as described (DiBartolomeis et al., 1986). After TCDD treatment (10 nM, 24 h), treatment media were removed from the cells and were replaced with fresh media containing the substrate DMBA (10 μM) and incubated for varying times depending on the cell activity. Media were collected from cells for DMBA metabolite analysis, and the cells were trypsinized and counted. The media/metabolites were treated with 0.1 μM β-glucuronidase for 1 h at 37°C. Metabolites were extracted in ethyl acetate/acetone mixture (2:1 ratio) containing 1 mM DTT and were separated and quantified by reverse-phase HPLC.

Enzyme Activity in Microsomal Preparations. Microsomal fractions from control or TCDD-treated cells (10 nM, 24 h) were isolated for Western immunoblotting and enzyme activity measurements. DMBA metabolism was measured in microsomal preparations as described (Pottenger and Jefcoate, 1990). The reaction mixtures contained 50 mM potassium phosphate buffer (pH 7.5), 3 mM $MgCl_2$, and NADPH-generating system (60 mM glucose 6-phosphate, 5 mM NADP, and 0.5 U/ml glucose-6-phosphate dehydrogenase). Samples (in duplicates) were preincubated 1 min at 37°C, and the reaction was initiated by the addition of 15 μM DMBA. The reaction was terminated after 10 min by the addition of ethyl acetate/acetone (2:1 ratio) containing 1 mM DTT, and metabolites were extracted and analyzed by reverse-phase HPLC as described previously (Christou et al., 1989).

Electrophoresis and Immunoblotting. Protein samples were solubilized in SDS-electrophoresis sample buffer containing 20 mM DTT, boiled for 5 min, and centrifuged briefly before being electrophoresed on 7.5% polyacrylamide gels as described (Laemmli, 1970). For immunoblotting, proteins were electrotransferred from acrylamide gels to nitrocellulose membrane, which was then blocked in 5% nonfat dry milk in Tris-buffered saline (pH 8.0) containing 0.05% Tween-20. Membranes were washed in Tris-buffered saline (pH 8.0) containing 0.05% Tween-20 and incubated with rabbit anti-CYP1B1, anti-CYP1A1, anti ARNT, or anti-AhR antibodies for 2 h. The anti-rabbit IgG-horseradish peroxidase conjugate served as the secondary antibody at a 1:20,000 dilution. Immunoreactive proteins were visualized by the enhanced chemiluminescence (ECL) procedure according to the manufacturer's protocol (Amersham Life Science, Arlington Heights, IL). The AhR and ARNT proteins were detected by polyclonal antibodies raised to AhR or ARNT fusion proteins, respectively (Pollenz et al., 1994). The specific immunodetectable CYP1A1 and CYP1B1 protein bands were quantified by densitometric scanning of the blots as described above for PCR images using microsomes from Hepa-1 WT and 10T1/2 cells, respectively, as standards.

Results

To establish the regulation of CYP1B1 relative to CYP1A1 by the AhR, we examined their expression in wild-type mouse hepatoma cells, Hepa-1c1c7, and its variant cell lines LA1 and LA2. These cell lines have been used extensively to study the mechanisms of AhR-dependent induction of CYP1A1 (Legraverend et al., 1982; Miller et al., 1983). CYP1B1 is not measurable in Hepa-1 cell lines by Northern analysis; however, RT-PCR using specific CYP1B1 primers generates a product of expected size. The identity of the PCR-amplified fragments was confirmed by Southern blotting via hybridization with a P^{32}-labeled CYP1B1 cDNA probe. The RT-PCR quantitation of the relative levels of CYP1B1 and CYP1A1 mRNAs was standardized by serial dilution (Fig. 1), as described inr *Materials and Methods*. The relative values generated by RT-PCR were validated against values from Northern blot analysis of CYP1B1 and CYP1A1 mRNAs in 10T1/2 and Hepa-1 cells, respectively (data not shown), and they also were comparable to published data for

CYP1A1 and CYP1B1 in these two cell lines (Savas et al., 1994).

PCR analyses of CYP1A1 and CYP1B1 expression in Hepa-1 and 10T1/2 cells demonstrated the cell-specific expression of CYP1A1 and CYP1B1 in Hepa-1 and 10T1/2 cell lines, respectively (Fig. 2 and Table 4). Whereas the TCDD-induced CYP1B1 mRNA level was approximately 100-fold higher in 10T1/2 than in Hepa-1 cells, the level of TCDD-induced CYP1A1 mRNA in Hepa-1 WT cells was about 300-fold higher than in 10T1/2. This difference between the two cell types is because of a 100-fold difference in their basal expression of CYP1B1 and CYP1A1 mRNA rather than a difference in induction factor. At the apoprotein level, TCDD-induced Hepa-1 WT expressed 200-fold-lower CYP1B1 than 10T1/2 cells where we detected about 30 pmol/mg microsomal protein, as quantified relative to an *Escherichia coli*-expressed recombinant mouse CYP1B1 (Fig. 3A and Table 4).

Before using the Hepa-1 wild-type and variant cell lines, their AhR signal components were verified by immunoblot analysis of Trizol-protein extract of control or TCDD-treated

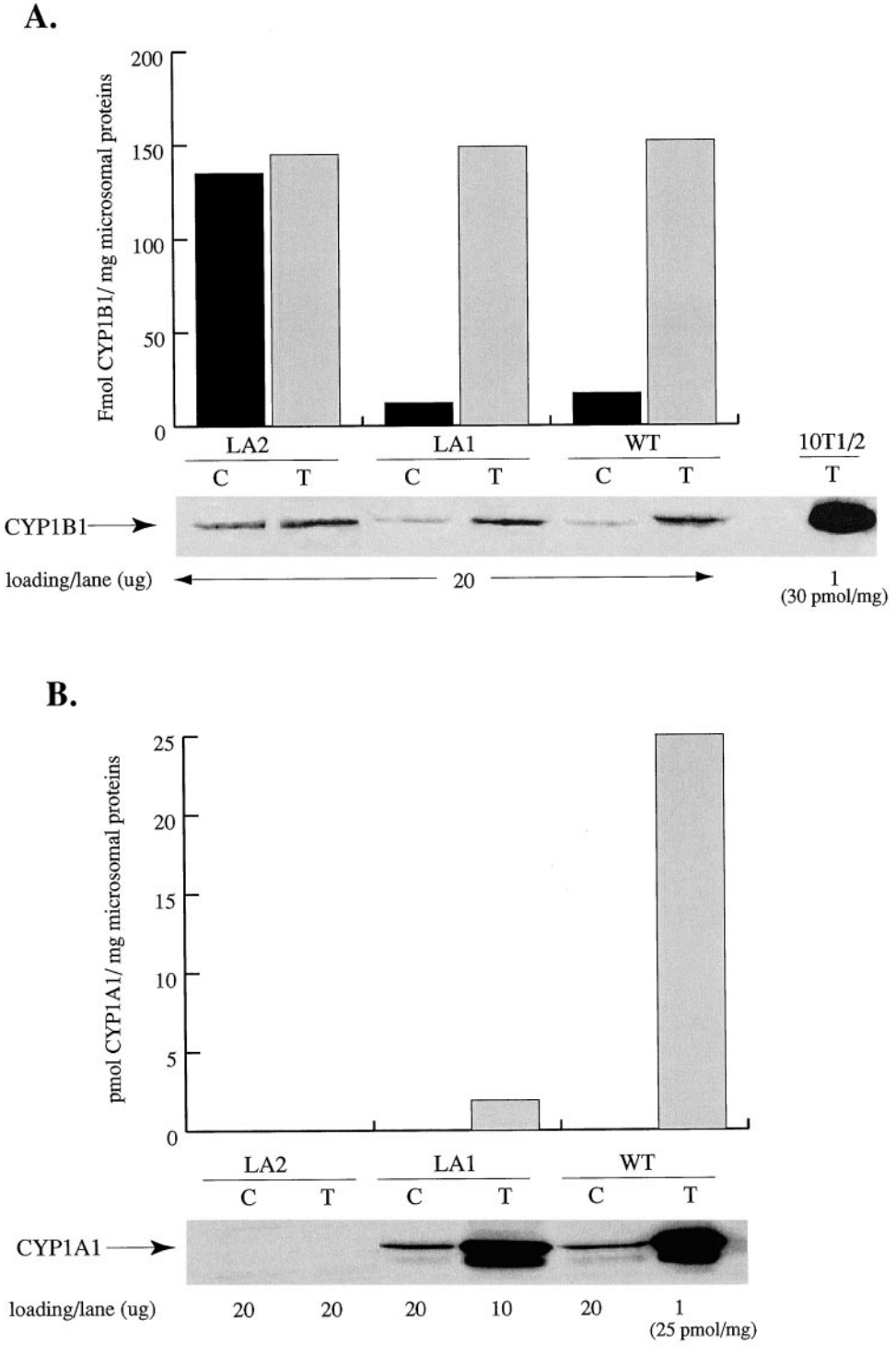

Fig. 3. Western immunoblot analysis of CYP1A1 and CYP1B1 in Hepa-1 cell lines after treatment with 10 nM TCDD for 24 h. Indicated amounts of microsomal proteins from treated cell lines were resolved on 7.5% SDS-PAGE and transferred to nitrocellulose membranes. membranes were probed with anti-CYP1B1 (A) or anti-CYP1A1 (B) polyclonal antibodies. goat anti-rabbit-horseradish peroxidase conjugate was used as secondary antibody at 1:20,000 dilution. Visualization of immunoreactive proteins was done by ECL system (Amersham). One microgram of microsomal proteins from TCDD-treated 10T1/2 cell lines was run as a positive control for CYP1B1 quantitation. relative intensity of specific protein bands was quantified by digital scanning of shorter exposure blot images and quantified relative to microsomal protein from TCDD-treated 10T1/2 cells (specific activity: 30 pmol CYP1B1/mg protein) and TCDD-treated Hepa-1 cells (specific activity: 25 pmol CYP1A1/mg protein). Values obtained were corrected for protein loading and are presented in bar graph above corresponding gel image.

cells. The results presented in Fig. 4A confirmed that the level of AhR protein in both the WT and LA2 variant was 10-fold higher than in the LA1 variant. Furthermore, the treatment with TCDD for 2 h resulted in substantial down-regulation of the receptor protein in WT and LA1 cells, consistent with published reports (Prokipcak and Okey, 1991; Pollenz, 1996). No down-regulation of AhR by TCDD treatment was observed in LA2. On the other hand, ARNT protein was not detectable in LA2 variant, whereas it was expressed at substantial levels in the WT and LA1 cells (Fig. 4A).

The basal CYP1A1 mRNA expression in LA1 (low-AhR-Hepa variant) was only slightly lower than WT, and 18-h treatment with TCDD unexpectedly resulted in the induction of CYP1A1 mRNA in LA1 cells to about 60–80% of the level in induced WT cells (Fig. 4B and Table 5). The expression of basal and BA- and TCDD-induced CYP1B1 in LA1 followed the same pattern of CYP1A1, attaining about 80% of the WT levels for either treatment (Fig. 4B and Table 5).

The induction of CYP1A1 protein and activity in Hepa WT cells paralleled that of mRNA. Western blot analysis for the apoprotein expression in Hepa-1 cell lines showed that 24-h TCDD treatment resulted in ~600-fold induction of CYP1A1 protein in WT cells (Fig. 3B). This corresponded to 500- and 200-fold induction in the enzymatic activity in whole-cell or isolated-microsome assay, respectively, as measured by DMBA metabolism (Table 6). However, TCDD induction of CYP1A1 protein and activity in LA1 cells showed a substantial discrepancy from the induction of its mRNA. In spite of near-comparable to WT steady-state mRNA levels, TCDD-induced LA1 cells exhibited only 10% of WT levels of CYP1A1 protein (Fig. 3B) and its associated DMBA metabolism (Table 6). Basal expression of CYP1A1 protein in the LA1 variant was similar to that in WT cells, consistent with the relative basal levels of CYP1A1 mRNA (Fig. 4B). CYP1B1 protein levels, on the other hand, were less responsive to TCDD than CYP1A1 with an average induction factor of 10 in WT and LA1 cells. However, unlike CYP1A1, the low but similar levels of CYP1B1 protein in the WT and LA1 cells (Fig. 3A) parallels the induction of CYP1B1 mRNA described in Fig. 4B and Table 5 and contrasts with an apparent suppression of CYP1A1 translation and/or reduced protein stability during PAH induction in LA1 cells.

Although the pattern of expression of CYP1B1 parallels that of CYP1A1 in both the Hepa-1 WT and LA1 variant, the expression of CYP1A1 and CYP1B1 diverged in the LA2 variant, which is deficient in ARNT protein (Fig. 4A) and lacks the TCDD-induced expression of CYP1A1 (Fig. 4B). This variant, however, expressed CYP1B1 mRNA basally at a level similar to the TCDD-induced WT level, and this basal CYP1B1 was not responsive to induction by TCDD or BA (Fig. 4B and Table 5). Western blot analysis confirmed, at the protein level, the elevated basal expression of CYP1B1 in

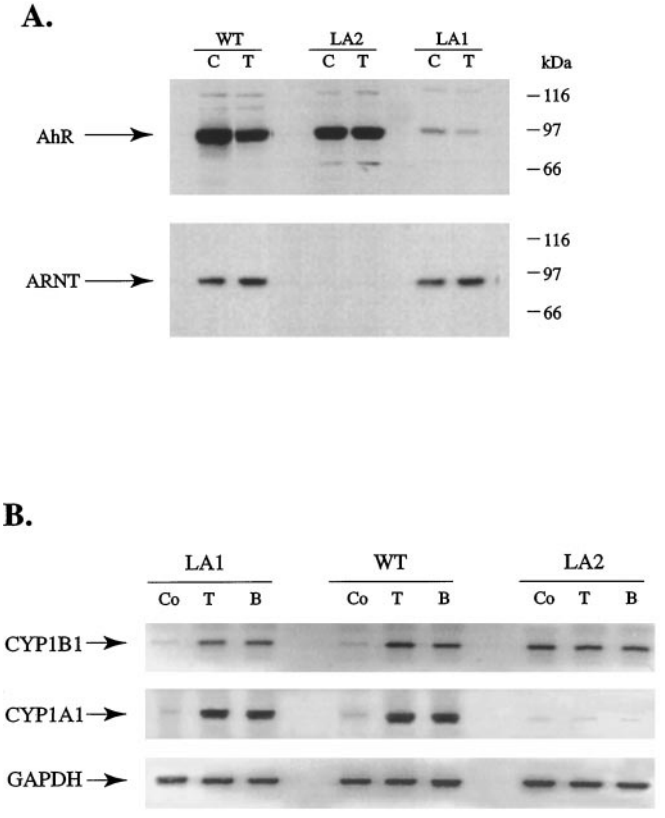

Fig. 4. A, Western immunoblot analysis of AhR and ARNT in Hepa-1 WT and variants. Total cellular proteins were isolated from Trizol lysate of cells treated with 10 nM TCDD or DMSO for 2 h. Equivalent amounts of proteins were resolved on 7.5% SDS-polyacrylamide gels and transferred to nitrocellulose membranes. membranes first were probed with anti-AhR antibodies and then stripped and reprobed with anti-ARNT antibodies. Visualization of immunoreactive proteins was done by ECL system (Amersham). B, representative negative film image of ethidium bromide-stained gel of RT-PCR-amplified CYP1A1 and CYP1B1 mRNA in Hepa-1 cell lines treated for 18 h with 10 nM TCDD (T), 10 μM benz[*a*]anthracene (B), or DMSO (Co). Equivalent RNA amounts from each cell line were subjected to RT reaction and subsequent PCR amplification (CYP1A1 for 25 cycles; CYP1B1 for 35 cycles), as described under *Materials and Methods* and Table 2. Similar gel images were scanned and quantified by digital scanning and normalized to their GAPDH values to obtain data presented in Table 5.

TABLE 5

Relative expression of CYP1A1 and CYP1B1 mRNA in Hepa-1 cell lines after treatment with TCDD or BA for 18 h

Cell Line	Treatment	CYP1A1[a]	CYP1B1[a]
WT	Control	1[b]	1[b]
	TCDD	179 ± 31	20 ± 2.5
	BA	170 ± 17.3	19 ± 3.7
LA1	Control	0.8 ± 0.4	0.5 ± 0.2
	TCDD	115 ± 26	16 ± 1.6
	BA	111 ± 18	15 ± 3.4
LA2	Control	0.6 ± 0.2	17 ± 2.4
	TCDD	0.5 ± 0.2	15 ± 1.8
	BA	0.4 ± 0.3	16 ± 2.2

[a] Mean and S.D. of three PCR determinations. Each determination was obtained by quantifying gel images such as in Fig. 4B, using standard curves similar to the one in Fig. 1. All values were normalized to GAPDH expression levels.
[b] Relative to control WT, which is defined as 1 for either CYP1A1 or CYP1B1.

TABLE 6

Total DMBA metabolism in whole-cell culture or in microsomal preparations of Hepa-1 cell lines after treatment with 10 nM TCDD for 24 h

Cell Line Treatment	*pmol/10^6 Cell/h*[a]	*pmol/mg Microsomal Protein/h*[a]
WT-Control	2.2 ± 0.3	44 ± 2
WT-TCDD	1154 ± 4.3	8770 ± 35
LA2-Control	N.D.	N.D.
LA2-TCDD	N.D.	N.D.
LA1-Control	1.7 ± 0.1	23 ± 1
LA1-TCDD	117 ± 6.6	678 ± 126

[a] Values are mean and S.D. of $n = 4$; duplicate assay of duplicate culture.
N.D., nondetectable.

LA2 cells (Fig. 3A). The data demonstrated that LA2 cells express CYP1B1 protein to the same level as TCDD-induced WT or LA1 cells. Although TCDD treatment for 24 h produced an ~10-fold induction over the basal level in WT and LA1 cells it did not affect the levels in LA2 cells. The level of CYP1B1 protein in Hepa cells, however, was too low to contribute any measurable activity toward DMBA metabolism in these cells, which exhibits a typical CYP1A1 metabolite profile (Table 6).

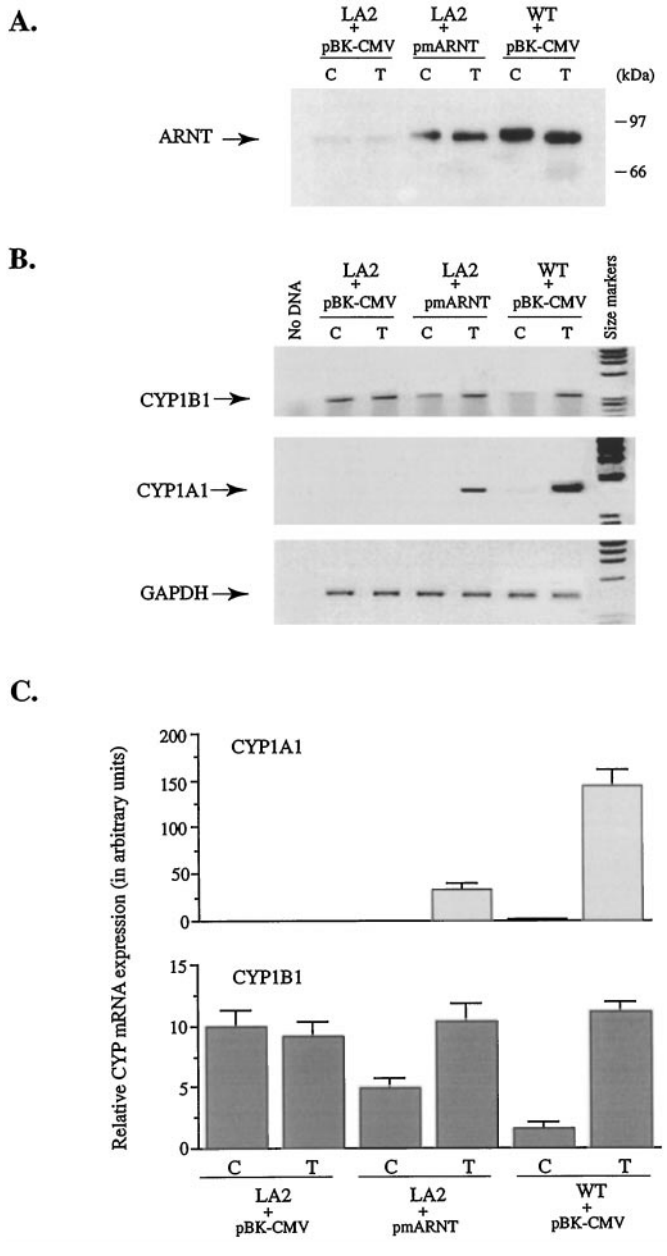

Fig. 5. Transient transfection of ARNT cDNA in LA2 Hepa-1 variant. Cells at subconfluency were transfected with either pmARNT (in LA2 cells) or pBK-CMV vector with no ARNT cDNA insert (in LA2 and WT cells) by electroporation as describe under *Materials and Methods*. Transfected cells were plated and allowed to recover for 24 h and then treated with 1 nM TCDD for 24 h. Cells were lysed in Trizol, and lysates were used for isolation of total RNA and protein. Proteins were analyzed by Western blotting using anti-ARNT antibodies to verify expression of ARNT protein in transfected cells (A). Equivalent amounts of RNA from WT, LA2, or ARNT-transfected LA2 cells were analyzed for CYP1B1 and CYP1A1 mRNA by RT-PCR. B, Representative negative image of ethidium bromide-stained gels of PCR-amplified products of basal and TCDD-induced CYP1B1 and CYP1A1 mRNA in WT, LA2, and ARNT-transfected LA2 cell lines. GAPDH was amplified as an internal control for normalization. Gel images of duplicate PCR determinations of duplicate cultures were scanned digitally and quantified as described under *Materials and Methods* using a dilution calibration curve as shown in Fig. 1. Means and S.D. of four determinations were plotted as a bar graph (C).

To directly address the role of ARNT in CYP1B1 mRNA expression, LA2 cells were transiently transfected with a plasmid containing ARNT cDNA. To obtain a high proportion of transfected cells, it was necessary to use strong electroporation conditions, which sacrificed about half of the cells; however, we were successful in achieving a very high transfection efficiency, resulting in the expression of approximately 45% of the WT levels of ARNT protein in surviving transfected LA2 cells (Fig. 5A). We verified that this cytotoxicity was not specific to the cells and was seen when the high-voltage pulse was used without DNA. The introduction of ARNT into LA2 mutant cells has resulted in the restoration of their TCDD-induced CYP1A1 mRNA expression from zero to a level equivalent to 25% of TCDD-induced WT cells (Fig. 5, B and C). This was accompanied by a repression in the basal expression of CYP1B1 mRNA in these ARNT-transfected LA2 cells to almost 50% of the level of their vector-transfected controls. This repressed expression, however, remained three times higher than the low WT basal levels. Thus, the reconstitution of the basal CYP1B1 repression in ARNT-transfected LA2 variant cells is comparable in effectiveness to the magnitude of the restoration of CYP1A1 induction in these cells (Fig. 5, B and C) and is approximately proportional to the increase in ARNT expression.

We next tested the effect of transfected ARNT on *CYP1B1* promoter activity. A luciferase reporter construct of the minimum 5′ flanking regulatory sequence of CYP1B1 gene (−1075/+150) was designed to include the enhancer and proximal promoter regions (Fig. 6A). The basal activity of this luciferase construct in WT was comparable to that in LA2 cells. TCDD treatment resulted in about a 3-fold induction in WT with no equivalent effect in the LA2 variant (Fig. 6B). Basal expression and TCDD induction of *CYP1B1*-luciferase activity in LA2 were enhanced 2- and 3.5-fold, respectively, after cotransfection of ARNT cDNA into these cells (Fig. 6B). Transfection of a deletion construct that contains the proximal promoter and part of an inhibitory region (−432/+124) resulted in a 4- to 5-fold increased luciferase activity in LA2 cells compared with transfection in WT Hepa cells (Fig. 6C). The same segment of *CYP1B1* promoter showed only minimal basal activity in WT cells because of the effect of an inhibitory region (Zhang et al., 1998). This elevated activity in ARNT-deficient LA2 cells suggests that ARNT has a negative effect on this proximal region, which contrasts with the stimulatory effect on the enhancer (−1075 to 810) in LA2.

Previous work with 10T1/2 cells (Zhang et al., 1998) has established that the upstream enhancer of *CYP1B1* (−1085 to 810) contains two anomalous types of XREs in addition to a typical XRE that shows TCDD-inducible AhR-ARNT complex (Table 3). Two elements (XRE1/2 and XRE4) form TCDD-independent complexes of the same size as the typical XRE5-AhR-ARNT complex. A third element, XRE3, forms a complex with a faster mobility. This previous work showed that these complexes were retained in comparable $AhR^{-/-}$ cells, indicating that the complexes do not contain AhR. To test the possibility that these complexes may involve ARNT

in combination with some other bHLH proteins, we carried out EMSA with nuclear extracts from WT and LA2 cells. Figure 7 shows that these complexes form to the same extent in WT and LA2 cells, suggesting that they also do not involve ARNT. Supershift experiments were done with anti-AhR and anti-ARNT antibodies. Figure 8A shows supershift comparisons of XRE4 and XRE5 complexes in WT cells. Under conditions in which the normal TCDD-sensitive XRE5 complex was supershifted completely by anti-AhR antibody, XRE4 was unaffected. In equivalent experiments with anti-ARNT, about 20% of XRE4 complex in WT was supershifted. This supershift also was seen in XRE4 complex with LA2 nuclear extracts (Fig. 8B). Because this complex also was formed in LA2 cells, this supershifted complex is unlikely to be a result of ARNT but, rather, reflects a cross-reacting ARNT-like protein. XRE3 showed no supershift with either antibodies, whereas XRE1/2 showed erratic partial shift with anti-ARNT.

Discussion

Using sensitive detection techniques, we have shown here that Hepa-1 cells express measurable amounts of TCDD-inducible CYP1B1 mRNA and protein, although maximum levels are about 100–200 times lower than in mouse C3H10T1/2 embryo fibroblasts. This CYP1B1 level represents less than 1% of total (CYP) in Hepa-1 cells, which express predominantly CYP1A1. In contrast, the main PAH-

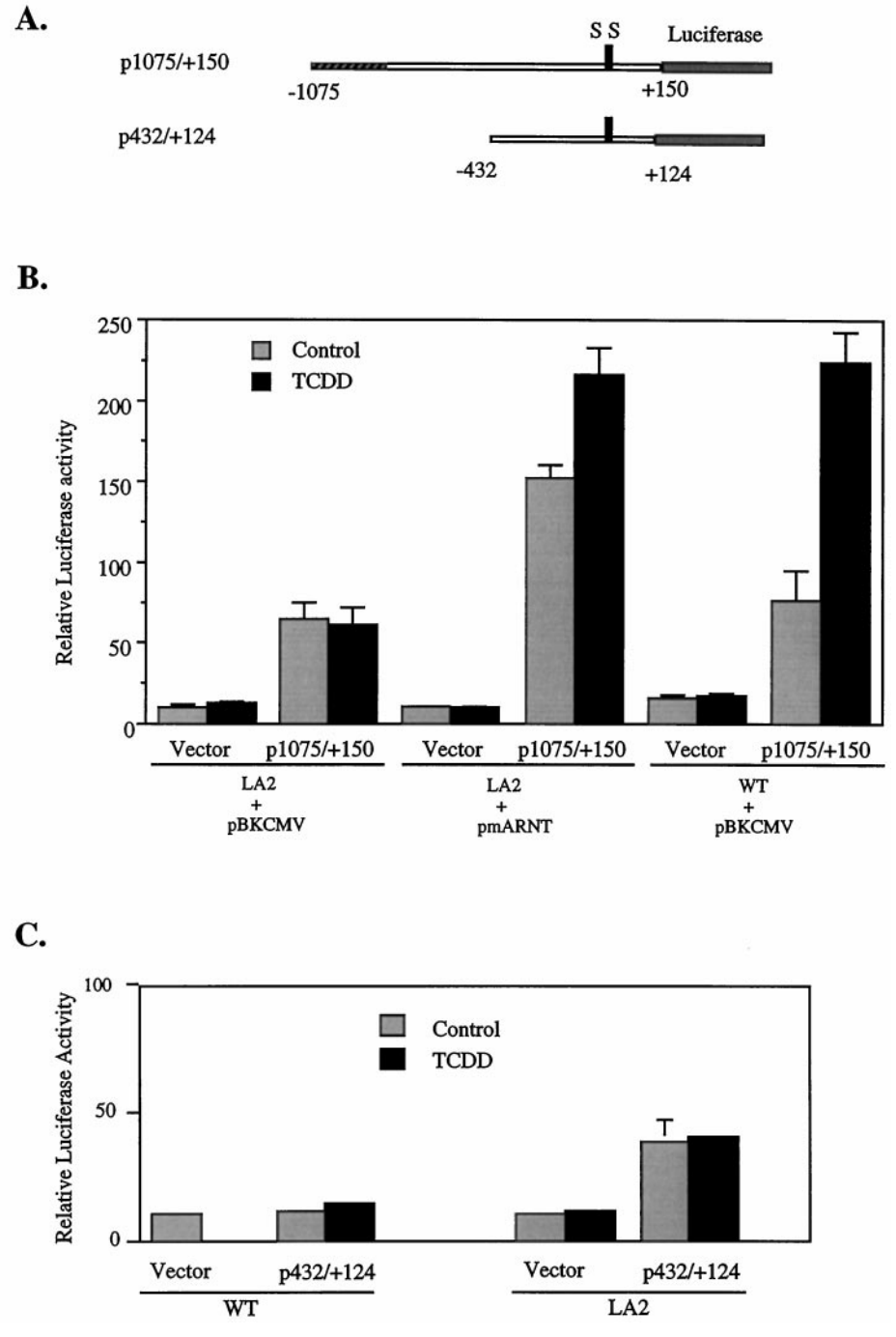

Fig. 6. Basal and TCDD induction of *CYP1B1*-luciferase constructs in WT and LA2 variant Hepa-1 cell lines. A, a full-length construct (−1075/+150) or a deletion construct (−432/+124) was transfected into Hepa-1 WT or LA2 variant. B, LA2 variants were cotransfected with (−1075/+150) construct and plasmid pmARNT containing mouse ARNT cDNA or, as a control, LA2 and WT cells were cotransfected with plasmid pBKCMV with no ARNT cDNA insert. C, WT or LA2 variant cells were transfected with deletion construct (−432/+124). Parallel pairs of transfection were done with pGL3Basic vector (without *CYP1B1* insert), and β-galactosidase expression vector pCH110 was cotransfected to control for transfection efficiency for both B and C. Luciferase activity was measured 48 h after transfection in presence or absence of TCDD treatment for 24 h. Luciferase activity was normalized to β-galactosidase activity, and relative luciferase activity was calculated as ratio of each activity to control vector activity (set as 10). Data represent mean ± S.E. of triplicate measurements from a single (C) or duplicate (B) experiments.

induced P-450 in C3H10T1/2 mouse fibroblast cell line is CYP1B1, whereas the cells express ~300-fold-lower CYP1A1 than Hepa-1 cells. We have shown that this cell specificity is related mainly to a difference in the basal expression of these two CYP genes, confirming our recent report using the transient transfection of luciferase-CYP1B1 enhancer constructs in Hepa-1 and 10T1/2 cells (Zhang et al., 1998). In spite of the enormous difference in expression level, the regulation of CYP1A1 and CYP1B1 mRNA maintains similar distinct features in Hepa-1 and 10T1/2 cells. CYP1B1 is less inducible by either TCDD or BA than CYP1A1 (10- versus 200-fold) in both Hepa cells and 10T1/2 cells because of a greater basal expression of CYP1B1. These data together with the parallel effects of AhR deficiency on the induction of both CYP1A1 and CYP1B1 mRNA in LA1 Hepa-1 mutant therefore suggest that the AhR mediates the induction of CYP1B1 by both TCDD and BA.

More detailed analysis has shown further points of similarity between CYP1A1 and CYP1B1 regulation that additionally provides a new perspective on AhR function. Whereas the initial rates of transcription of both *CYP1A1* and *CYP1B1* are very sensitive to the lower AhR levels in LA1 cells, which is evident by the very low mRNA expression at 3 h after TCDD treatment (S.E.E. and C.R.J., manuscript in preparation), the steady-state levels of both CYP1A1 and CYP1B1 mRNA expression after 18 h TCDD treatment are only ~25% lower in LA1 variants compared with the WT levels, which is disproportionate to the 10-fold-lower AhR level in LA1 cells. However, the previously reported (Miller et al., 1983; Hankinson et al., 1985) very low CYP1A1 protein and associated activity in LA1 cells was confirmed here and, therefore, could be arising from additional deficiency of translation in LA1 cells (Czaplinski et al., 1995). Noteworthy, however, is that the 10-fold-lower level of AhR in LA1 cells is similar to the AhR level observed in 10T1/2 cells (Pollenz, 1996), suggesting that the lower AhR level is accompanied by other inhibitory factors in LA1 cells. Clearly, differences between WT and the variant LA1 cells may arise from AhR-independent factors that have been selected into the variant line. However, recent work has established that AhR transfection is sufficient to reverse many differences in LA1 cells relative to WT (Ma and Whitlock, 1996; Weiss et al., 1996).

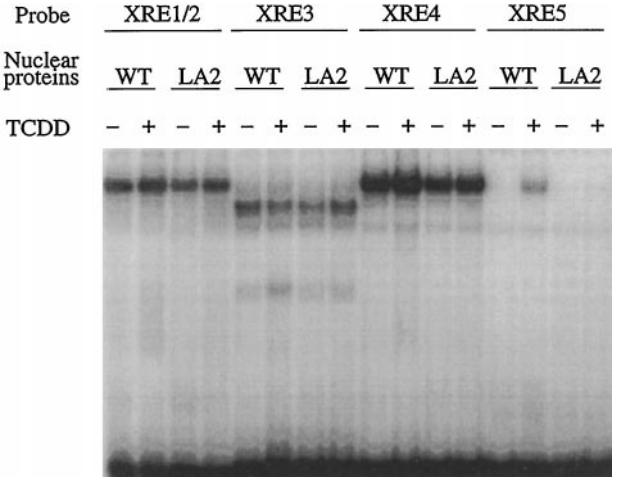

Fig. 7. Comparison of complexes formed between nuclear extracts from Hepa-1 WT or LA2 variant cells and four putative XRE sequences of *CYP1B1* gene. Nuclear extracts from untreated (−) and TCDD-treated (+) Hepa-1 WT or LA2 variant cells (1 nM, 2 h) were analyzed by gel mobility-shift assays using 30-mer oligonucleotides containing CYP1B1 enhancer putative XREs, sequences for which are outlined in Table 3.

We also have shown in this report that the regulation of CYP1B1 differs substantially from that of CYP1A1 in cells deficient in the AhR partner, ARNT. In the ARNT-deficient LA2 Hepa variant, unlike CYP1A1, CYP1B1 is constitutively expressed at levels approximating TCDD-induced WT levels, suggesting that AhR or other nuclear factor(s) are more effective in the absence of ARNT. Moreover, transient transfection of ARNT cDNA in LA2 variant cells has resulted in about a 50% lowering of the basal CYP1B1 mRNA, further supporting the inhibitory effect of ARNT on *CYP1B1* transcription. Analysis of the 5′ regulatory sequences of the *CYP1B1* gene in LA2 Hepa variant compared with WT revealed major differences between these two lines. Hepa WT cells exhibited both basal and TCDD-induced activity when transiently transfected with a *CYP1B1*-luciferase construct containing extended promoter and enhancer regions, whereas no TCDD-induced activity was produced in LA2 variant. The reversal of this response in LA2 by cotransfection of ARNT cDNA is consistent with the requirement for a functional ARNT in driving TCDD-induced activity (Probst et al., 1993). The enhancement of basal and TCDD-induced activity of this reporter construct by cotransfecting ARNT in LA2 cells is analogous to responses observed with the same promoter constructs in embryo fibroblasts derived from AhR knock-out mice ($AhR^{-/-}$) (Zhang et al., 1998).

However, these results with the promoter constructs are inconsistent with the regulation of the *CYP1B1* gene in LA2 cells. In these cells the basal activity of the *CYP1B1* gene is at the TCDD-induced WT levels and is suppressed by transfection of ARNT, whereas the high activity in TCDD-treated cells is not affected. However, we also have seen that the transient transfection of luciferase reporter constructs of *CYP1B1* and *CYP1A1* does not reproduce the cell selectivity of these genes in 10T1/2 and Hepa-1 cells and that the transient transfection of AhR produces an abnormal substantial basal luciferase activity (Zhang et al., 1998). Such discrepancies between the behavior of transiently transfected reporter construct plasmids and the native gene in its chromosomal setting are likely to be a result of factors related to the chromatin structure of these genes. The structure of chromatin is known to greatly influence the mammalian gene. Although we have not studied this aspect of regulation for *CYP1B1*, the enhancer/promoter region of *CYP1A1* in uninduced mouse hepatoma cells is inactive because of a repressive nucleosomal interaction (Morgan and Whitlock, 1992). Therefore, during induction, regulatory proteins such as AhR/ARNT need both to access their recognition sites within chromatin and to overcome the repressive effects of nucleosomes before they stimulate the interaction of general transcription factors with the promoter to enhance transcription (Whitlock et al., 1996). In nonnucleosomal templates such as transiently transfected reporter plasmids, there is less tight regulation where the primary function of AhR/ARNT during induction is to bind directly to their already accessible binding sites and recruit other general transcription factors to the wide-open, accessible promoter. Therefore, the inconsistent promoter construct data would imply that the chromatin structure plays a major role in the tight regulation of *CYP1B1* gene.

The transfection of a deletion construct (−432/+124) that spans the proximal promoter, a putative E-box, and four putative XRE-binding sites of *CYP1B1* gene resulted in an approximately 5-fold increase in the basal transcription of the luciferase reporter gene in LA2 cells relative to the basal activity in WT Hepa cells. This suggests that ARNT suppresses the proximal promoter activity in Hepa-1 cells. Analogous proximal *CYP1B1* promoter, which contains a putative XRE element, is maximally active in uninduced embryo fibroblasts derived from AhR knock-out mice ($AhR^{-/-}$), but is repressed by transfection of AhR in these cells (L. Zhang and C. R. Jefcoate, unpublished data). Together, these data suggest that ARNT in combination with AhR suppress proximal promoter activity, presumably acting at some regulatory elements in the proximal promoter region. Several negative regulatory sequences have been identified in the *CYP1B1* upstream region between the promoter and TCDD-responsive enhancer regions (Zhang et al., 1998). Evidently, the overall *CYP1B1* promoter activity is determined by a balance between positive and negative effects of AhR and ARNT proteins.

Like CYP1A1, the TCDD induction of CYP1B1 is mediated by an enhancer region containing a cluster of four XRE elements 1000 bp upstream from the transcription start site. Recent work in this laboratory has demonstrated that there are substantial differences between the two genes; for instance, unlike in *CYP1A1*, the enhancer region in *CYP1B1* seems to be more responsive to basal levels of AhR. We have identified previously in mouse embryo fibroblasts three non-TCDD-inducible-type complexes with three different consensus XREs of the *CYP1B1* gene, none of which are sensitive to the lack of AhR in embryo fibroblasts derived from AhR knock-out mice (Zhang et al., 1998). Here we show that these complexes do not interact with anti-AhR antibodies, further supporting the absence of AhR in these complexes. We have demonstrated here that the three complexes also are formed in LA2 cells in the absence of a functional ARNT. This confirms that these TCDD-insensitive complexes at *CYP1B1*

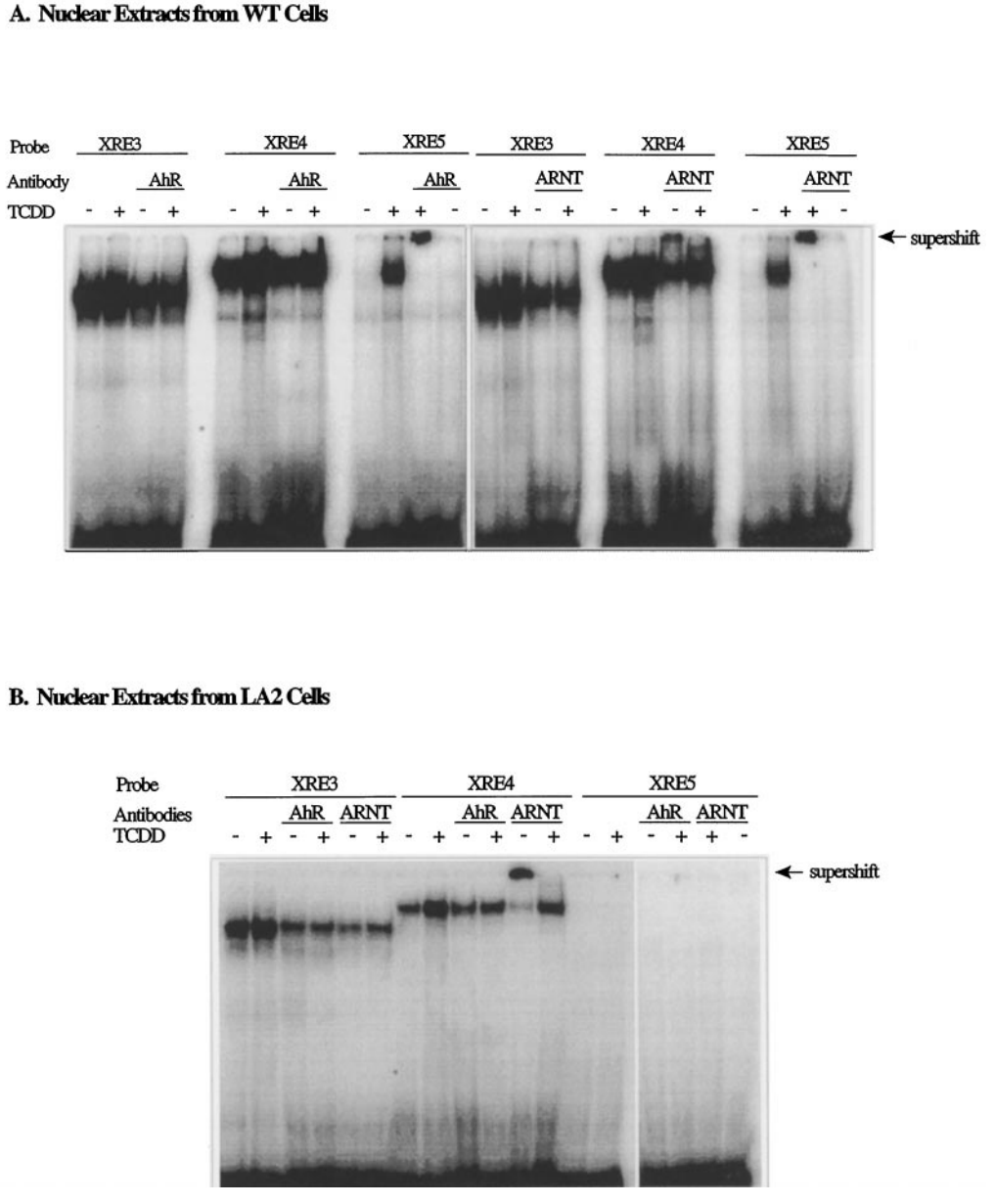

Fig. 8. A, effect of anti-AhR and anti-ARNT antibodies on complexes formed between nuclear extracts from Hepa-1 WT cells and tested XREs. Arrow denotes complexes supershifted by antibodies. B, effect of anti-AhR and anti-ARNT antibodies on formed complexes between nuclear extracts from LA2 variant cells and four XREs. Arrow points to supershifted XRE4 complex with anti-ARNT antibodies. In all cases, antibody incubations followed binding of nuclear extracts to oligonucleotides.

XREs do not involve AhR or ARNT. This is somewhat surprising because the size of the complexes at XRE1/2 and XRE4 is indistinguishable from that of the ARNT-AhR complex at XRE5. The anti-ARNT antibodies did partially modify the formation of the XRE4 complexes in LA2 and WT cells. However, we have detected in LA2 cells a protein of the same size as ARNT that weakly cross-reacts with anti-ARNT antibodies on immunoblots (Fig. 5A). Possibly, LA2 cells express an ARNT-like protein that, although nonfunctional in translocating AhR and dimerizing with it, is capable of DNA binding in cooperation with other partners. Some recently identified members of the PAS/bHLH family, such as ARNT2, murine sim1, or sim2, fit these criteria (Ema et al., 1996; Hirose et al., 1996). Further investigation is required to verify the identity and function of this ARNT-like protein in LA2. It is possible that under basal conditions in LA2 cells this protein dimerizes with any of the PAS/bHLH proteins (except AhR) and exerts transcriptional activation of *CYP1B1* by binding to a consensus motif such as E-box (Antonsson et al., 1995).

Acknowledgments

We thank Dr. Richard Pollenz (University of South Carolina, Charleston) for generously providing the anti-AhR and anti-ARNT antibodies, Drs. Üzen Savas and Carsten Carstens for technical advice on RT-PCR, and Dr. Michele Larsen for editing the manuscript.

References

Antonsson C, Arulampalam V, Whitelaw ML, Pettersson S and Poellinger L (1995) Constitutive function of the basic-helix-loop helix/PAS factor Arnt. Regulation of target promoters via the E box motif. *J Biol Chem* **270:**13968–13972.

Bhattacharyya K, Brake P, Eltom SE, Otto S and Jefcoate CR (1995) Identification of a rat adrenal cytochrome P450 active in polycyclic hydrocarbon metabolism as rat CYP1B1. Demonstration of a unique tissue-specific pattern of hormonal and aryl hydrocarbon receptor-linked regulation. *J Biol Chem* **270:**11595–11602.

Burback KM, Poland AP and Bradfield CA (1992) Cloning of the Ah receptor cDNA reveals a distinctive ligand-activated transcription factor. *Proc Natl Acad Sci USA* **89:**8185–8989.

Chomcynski P (1993) A reagent for the single step simultaneous isolation of RNA, DNA and proteins from cells and tissue samples. *BioTechniques* **15:**532–537.

Christou M, Jovanovich MC and Jefcoate CR (1989) Epoxide hydratase: Sex specific expression and rate limiting role in DMBA metabolism. *Carcinogenesis* **10:**1883–1890.

Christou M, Savas U, Schroeder S, Shen X, Thompson T, Gould MN and Jefcoate CR (1995) Cytochrome CYP1A1 and CYP1B1 in the rat mammary gland: Cell-specific expression and regulation by polycyclic aromatic hydrocarbons and hormones. *Mol Cell Endocrinol* **115:**41–50.

Czaplinski K, Weng Y, Hagan KW and Peltz SW (1995) Purification and characterization of the Upf1 protein: A factor involved in translation and mRNA degradation. *RNA* **1:**610–623.

Denison MS, Fisher JM and Whitlock JP Jr (1989) Protein-DNA interactions at recognition sites for the dioxin-Ah receptor complex. *J Biol Chem* **264:**16478–16482.

DiBartolomeis MJ, Christou M and Jefcoate CR (1986) Regulation of rat and bovine adrenal metabolism of polycyclic aromatic hydrocarbons by adrenocorticotropin and 2,3,7,8-tetrachlorodibenzo-p-dioxin. *Arch Biochem Biophys* **46:**428–438.

Eltom SE, Larsen M and Jefcoate CR (1998) Expression of CYP1B1 but not CYP1A1 by primary cultured human mammary fibroblasts constitutively and in response to dioxin: Role of the Ah receptor regulation. *Carcinogenesis* **19:**1437–1444.

Ema M, Morita M, Ikawa S, Tanaka M, Mastsuda Y, Goto O, Saijoh Y, Fujii H, Hamada H, Kikuchi Y and Fujii-Kuriyama Y (1996) Two new members of the murine sim gene family are transcriptionally repressor and show different expression patterns during mouse embryogenesis. *Mol Cell Biol* **16:**5865–5875.

Fort P, Marty L, Piechaczyk M, El Sabrouty S, Dani C, Jeanteur P and Blanchard JM (1985) Various rat adult tissues express only one major mRNA species from the glyceraldehyde-3-phosphate dehydrogenase multigenic family. *Nucleic Acids Res* **13:**1431–1442.

Gonzalez FJ, Mackenzie PI, Kimura S and Nebert DW (1984) Isolation and characterization of full-length mouse cDNA and genomic clones of 3-methylcholanthrene-inducible cytochrome P_1-450 and P_3-450. *Gene* **29:**281–292.

Hankinson O, Andersen RD, Birren DW, Sander F, Negishi M and Nebert DW (1985) Mutations affecting the regulation of transcription of the cytochrome P1–450 gene in the mouse Hepa-1 cell line. *J Biol Chem* **260:**1790–1795.

Hirose K, Morita M, Ema M, Mimura J, Hamada H, Fuji H, Saijo Y, Goto O, Sogawa K and Fujii-Kuriyama Y (1996) cDNA cloning and tissue-specific expression of a novel basic helix-loop-helix/PAS factor (Arnt 2) with close sequence similarity to the aryl hydrocarbon receptor nuclear translocator (Arnt). *Mol Cell Biol* **16:**1706–1713.

Hoffman EC, Reyes H, Chu F-F, Sander F, Conley LH, Brooks BA and Hankinson O (1991) Cloning of a factor required for activity of the Ah (dioxin) receptor. *Science* **252:**954–958.

Jones PB, Galeazzi DR, Fisher JM and Whitlock JP Jr (1985) Control of cytochrome P_1-450 gene expression by dioxin. *Science* **227:**1499–1502.

Laemmli UK (1970) Cleavage of structural proteins during the assembly of the head of bacteriophage T4. *Nature (London)* **227:**680–685.

Legraverend C, Hannah RR, Eisen HJ, Owens IS, Nebert DW and Hankinson O (1982) Regulatory gene product of the Ah locus: Characterization of receptor mutants among mouse hepatoma clones. *J Biol Chem* **257:**6402–6407.

Ma Q and Whitlock, JP Jr (1996) The aromatic hydrocarbon receptor modulates the Hepa-1c1c7 cell cycle and differentiated state independently of dioxin. *Mol Cell Biol* **16:**2144–2150.

Miller AG, Israel D and Whitlock J P Jr (1983) Biochemical and genetic analysis of variant mouse hepatoma cells defective in the induction of benzo(a)pyrene-metabolizing enzyme activity. *J Biol Chem* **258:**3523–3527.

Morgan JE and Whitlock J P Jr (1992) Transcription-dependent and transcription-independent nucleosome disruption induced by dioxin. *Proc Natl Acad Sci USA* **89:**11622–11626.

Otto S, Marcus C, Pidgeon C and Jefcoate CR (1991) A novel adrenocorticotropin-inducible cytochrome P450 from rat adrenal microsomes catalyze polycyclic aromatic hydrocarbon metabolism. *Endocrinology* **129:**970–998.

Pollenz RS (1996) The aryl-hydrocarbon receptor, but not the aryl-hydrocarbon receptor translocator protein, is rapidly depleted in hepatic and non-hepatic culture cells exposed to 2,3,7,8-tetrachlorodibenzo-p-dioxin. *Mol Pharmacol* **49:**391–398.

Pollenz RS, Sattler CA and Poland AP (1994) The aryl hydrocarbon receptor and aryl hydrocarbon receptor translocator protein show distinct subcellular localization in Hepa-1c1c7 cells by immunofluorescence microscopy. *Mol Pharmacol* **45:**425–428.

Pottenger LH, Christou M and Jefcoate CR (1991) Purification and immunological characterization of a novel cytochrome P450 from C3H/10T1/2 cells. *Arch Biochem Biophys* **286:**488–497.

Pottenger LH and Jefcoate CR (1990) Characterization of a novel cytochrome P450 from the transformable cell line, C3H/10T1/2. *Carcinogenesis* **11:**321–327.

Probst MR, Reisz-Porszasz S, Agbunag RV, Ong MS and Hankinson O (1993) Role of the aryl hydrocarbon receptor nuclear translocator protein in aryl hydrocarbon (dioxin) receptor action. *Mol Pharmacol* **44:**511–518.

Prokipcak RD and Okey AB (1991) Down regulation of the Ah receptor in mouse hepatoma cells treated in culture with 2,3,7,8-tetrachlorodibenzo-p-dioxin. *J Physiol Pharmacol* **69:**1204–1210.

Ryu DY, Levi PE, Fernandez-Salguero P, Gonzalez FJ, Hodgson E (1996) Piperonyl butoxide and acetuphthylene induces cytochrome P4501A2 and 1B1 mRNA in aromatic hydrocarbon-responsive receptor Knock-out mouse liver. *Mol Pharmacol* **50:**443–446.

Savas U, Bhattacharyya K, Christou M, Alexander D and Jefcoate CR (1994) Mouse cytochrome p450EF representative of a new 1B subfamily of cytochrome P450s. Cloning, sequence determination and tissue expression *J Biol Chem* **269:**14905–14911.

Savas U, Carstens CP and Jefcoate CR (1997) Biological oxidations and p450 reactions—Recombinant mouse CYP1B1 expressed in E. coli exhibits selective binding by polycyclic hydrocarbons and metabolism which parallels C3H10T1/2 cell microsomes but differs from human recombinant CYP1B1. *Arch Biochem Biophys* **347:**181–192.

Savas U and Jefcoate CR (1994) Dual regulation of cytochrome p450EF expression via the aryl hydrocarbon receptor and protein stabilization in C3H/10T1/2 cells. *Mol Pharmacol* **45:**1153–1159.

Shen Z, Wells RL, Liu J and Elkind MM (1993) Identification of a cytochrome P450 gene by reverse transcription-PCR using degenerate primers containing inosine. *Proc Natl Acad Sci USA* **90:**11483–11487.

Smith PK, Krohn RI, Hermanson GT, Mallia AK, Gartner FH, Provenzano MD, Fujimoto EK, Goeke NM, Olson BJ and Glenk DC (1985) Measurement of protein using bicinchoninic acid. *Anal Biochem* **150:**76–85, and erratum (1987) **163:**279.

Sutter TR, Tang YM, Hayes CL, Wo Y-Y, Jabs EW, Li X, Yin H, Cody CW and Greenlee WF (1994) Complete cDNA sequence of a human dioxin-inducible mRNA identifies a new gene subfamily of cytochrome P450 that maps to chromosome 2. *J Biol Chem* **269:**13092–13099.

Weiss C, Kolluri SK, Kiefer F and Gottlicher M (1996) Complementation of Ah receptor deficiency in hepatoma cells: Negative feedback regulation and cell cycle control by the Ah receptor. *Exp Cell Res* **226:**154–163.

Whitlock JP Jr, Okino ST, Dong L, Ko HP, Clarke-Katzenberg R, Ma Q and Li H (1996) Induction of cytochrome P4501A1: A model for analyzing mammalian gene transcription. *FASEB J* **10:**809–818.

Wislocki PG, Gadek KM, Chou MW, Yang SK and Lu AY (1980) Carcinogenicity and mutagenicity of the 3,4-dihydrodiols and other metabolites of 7,12-dimethylbenz(a)anthracene and its hydroxymethyl derivatives. *Cancer Res* **40:**3661–3664.

Zhang L, Savas U, Alexander D and Jefcoate CR (1998) Characterization of the mouse CYP1B1 gene: Identification of an enhancer region that directs aryl hydrocarbon receptor-mediated constitutive and induced expression. *J Biol Chem* **273:**5174–5183.

Send reprint requests to: Dr. Sakina E. Eltom, Department of Pharmacology, University of Wisconsin Medical School, 1300 University Ave., Madison, WI 53706. E-mail: seeltom@facstaff.wisc.edu